

# Two-Branch Microwave Channelized Active Bandpass Filters

Christen Rauscher, *Fellow, IEEE*

**Abstract**—The realization of small highly selective microwave filters has emerged as a prominent issue in the design of miniaturized high-frequency systems. In this paper, a new way to implement channelized active bandpass filters is presented that deals with the impasse. The concept involves a two-branch configuration, which yields filter circuits that are more compact and offer lower noise figures than earlier three-branch versions, while still retaining all the advantages of channelized feedforward operation. The practicability of the technique is demonstrated with two 10-GHz bandpass filters of different design, whose assessed performance characteristics include signal distortion and noise properties.

**Index Terms**—Channelized filter, microwave active filter, microwave band-reject filter, microwave low-distortion active filter, microwave low-noise active filter, microwave notch filter, miniature high-selectivity filter, miniature microwave filter.

## I. INTRODUCTION

CURRENT trends toward integrated multifunction systems for military applications have resulted in heightened demand for microwave filters that exhibit good frequency selectivity, yet are small in size. Selectivity requirements derive both from the need to isolate system functions being performed simultaneously in separate frequency bands, and from the necessity to limit external signal interference through control of receiver bandwidth. Size constraints are dictated, in part, by phased-array system concepts being developed, which restrict filter geometries to dimensions commensurate with the close spacing of array antenna elements. Miniature high-performance microwave filters find use in other applications as well, such as in mobile communication equipment and frequency-synthesized signal generators.

Microwave system designs have traditionally depended on passive-circuit filter implementations, involving tradeoffs between filter performance and size. There has been concurrent interest, though, in active-circuit alternatives, which promise solutions that may be less constrained by compromise. In these approaches, active circuit elements are used to compensate for the effects of passive-circuit losses on passband attenuation and frequency selectivity. The simplest approach is to utilize a cascade connection of passive filter segments and gain blocks. Although such a configuration offers compensation for the effects of passive-element losses on average passband transmission, it neither has the ability to efficiently counteract the effects of such

losses on filter flank steepness and passband shoulders, nor does it constitute a particularly attractive choice for achieving maximum frequency selectivity with a minimum number of circuit elements. Among the advantages of the cascade method are its design simplicity and a low sensitivity of filter characteristics to variations in circuit element values.

By far the most popular approach to microwave active filter design is to rely on transistors with regenerative feedback to provide  $Q$ -factor enhancement of passive circuit elements, thereby allowing, in contrast to the simple-cascade case, the integrity of passband edges and filter flanks to be retained in the presence of element losses. The resulting toleration of such losses permits highly selective filters to be realized in compact lumped-element form. Concerns about circuit stability and noise performance associated with regenerative feedback, however, have made system designers reluctant to embrace the concept. Technological advances in circuit fabrication and adaptive gain control are gradually changing this perception [1].

An alternate approach to coping with the effects of element losses on filter selectivity is to engage feedforward, rather than feedback methods. The analog transversal filter is a classic example, in which an incident signal is divided into a multiplicity of subcomponents that are individually amplitude weighted and time delayed before they are combined into a composite output signal. Filter action originates from constructive and destructive interference among the subcomponents. Through the avoidance of resonant circuit conditions, dissipation losses are not a major factor. Neither is circuit stability, due to the absence of feedback. The main disadvantages of analog transversal filters lie in the large amount of aggregate time delay and the large number of active-circuit weighting elements required to achieve good selectivity. Modified transversal filter architectures have been proposed, aimed at overcoming these impediments [2], [3], but still do not provide solutions that are practical for narrow-bandwidth applications. A wider range of filter design options are available by resorting to channelized active filters [4]. These distinguish themselves from transversal structures through the use of frequency-selective amplitude weighting, as opposed to frequency-independent weighting. The result is a significant reduction in the number of feedforward branches needed to achieve a specified transfer response, leading to compact high-selectivity filters that retain the principal benefits of transversal structures with regard to noise performance, circuit stability, and coping with passive-circuit transmission losses.

In a microwave channelized active filter, one of the parallel-connected branches normally serves as the main signal channel,

Manuscript received July 1, 1999; revised December 10, 1999. This work was supported by the Office of Naval Research.

The author is with the Naval Research Laboratory, Washington, DC 20375-5347 USA.

Publisher Item Identifier S 0018-9480(00)02071-8.

tasked with producing a low-order approximation of the specified filter response. Auxiliary channels are added to transform, through interference among signal components, the low-order approximation into a useful overall filter response. Low-pass, high-pass, and band-reject filters can be realized with a total of only two channels, whereas bandpass responses have required, to-date, a minimum of three. Although the three-to-two ratio may not seem all that significant, it does place bandpass implementations at a disadvantage with regard to design complexity, space requirements, prime-power consumption, and noise performance. The technique described below permits microwave channelized bandpass filters to also be realized with only two branches.

## II. THE CONCEPT

In a channelized filter, the frequency-selective branches supply the equivalent of complex-valued basis functions from which composite transfer characteristics are synthesized through vector summation. A typical bandpass configuration comprises a main branch with single-tuned bandpass transfer characteristics and two auxiliary branches of similar design with response peaks positioned in the vicinities of the composite filter's flanks, one on each side. Amplitude and phase relationships among channel transfer characteristics are engineered for mutual signal reinforcement across the passband to yield a well-behaved passband response. Stopband edges are defined by manipulating channel bandwidths and signal phase relationships so that branch signals cancel each other at frequencies where transmission nulls are desired. The channels' band-limited nature allows signals to change rapidly from in-phase conditions at the passband edges to out-of-phase conditions at the null frequencies, enabling sharp passband-to-stopband transitions. In determining filter flank steepness, channel amplitude selectivity is not as critical as signal phase relationships, mitigating concerns about passive-circuit losses associated with the frequency-selective branch networks.

With constant demands for ever smaller circuit dimensions, the notion of a more compact two-branch channelized bandpass filter option is an attractive proposition. Whereas signal interactions in the three-branch case concentrate on one filter flank at a time, encompassing the main channel and one of the auxiliary channels, the two-branch approach would invariably require that both channels be simultaneously engaged in the shaping of both filter flanks. Specifically, the two channel networks would have to be designed to not only accommodate signals that complement each other at passband frequencies to generate smooth passband characteristics, but also to destructively interfere with each other to create desirable transmission nulls at close-in stopband edges.

The compounded demands place strict constraints on channel amplitude and phase responses across the entire frequency span of interest. Relative signal phases must rotate through a total of  $360^\circ$  as signal interference proceeds from cancellation at one stopband edge, through reinforcement in the passband, to renewed cancellation at the other stopband edge. Applicable phase responses could be realized with conventional sections of delay

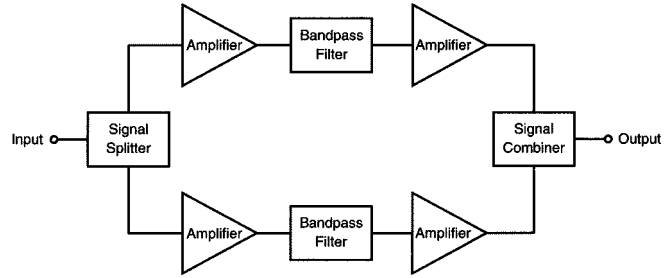


Fig. 1. Schematic block diagram of a two-branch microwave channelized bandpass filter employing an in-phase power splitter at the input and a power combiner at the output.

line. In narrow-band situations, however, where phase differentials must change very rapidly with frequency, pertinent sections would occupy too much space. A more efficient approach is to assign band-limited filter functions of different orders to each channel, chosen to generate, from one stopband edge to the other, the necessary  $360^\circ$  of differential transmission phase shift between channels.

The simplest way to implement a two-channel bandpass filter is with the help of an in-phase power splitter that divides the incident signal between the two branches, and an in-phase power combiner that merges the two branch signals back into one at the output after passing through respective channel networks. Each channel network may be configured as a cascade assembly of amplifiers and bandpass filter sections, with a typical arrangement depicted in Fig. 1. This arrangement is easy to realize, based on the fact that it is made up entirely of  $50\text{-}\Omega$ -referenced building blocks. With the noted toleration for passive-element losses, circuits can be made very compact through reliance on integrated lumped-element technology for signal splitters and combiners, filter sections, and amplifiers. A potential drawback of this particular implementation lies with its susceptibility to interference from out-of-band signals, as the input amplifiers are not preceded by a means of frequency preselection. Another potential concern is the fact that the two channels do not fully utilize their allocated shares of the input signal, as signal content that falls outside each channel's ascribed frequency response is discarded. The partial sacrifice of signal power is akin to adding attenuation at the input, which, in turn, affects minimum achievable noise-figure values. It should be noted, however, that the two-branch configuration still holds, in this regard, a significant 1.8-dB advantage over a comparable three-branch realization, as confirmed by computer simulations for cases where signal power is distributed equally among channels.

To address the dual issue of noise and susceptibility to interference, a frequency diplexer, instead of a power splitter, can be employed to separate an incident signal into two portions, as illustrated in Fig. 2. Conditions at the filter output are less critical than at the input, permitting either the use of an in-phase combiner at the output, as in the previous case, or another diplexer, as indicated in the figure. Unlike a conventional input diplexer, which is commonly used to partition the frequency content of an incident signal into two separate frequency bands, the arrangement needed here must be capable of dividing the signal between two bandpass channels whose passbands overlap, with

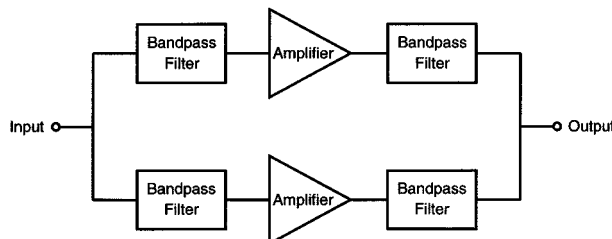


Fig. 2. Schematic block diagram of a two-branch microwave channelized bandpass filter employing input and output diplexer circuits.

the passband of one channel often fully contained within the passband of the other. Although channelized filters that rely on diplexers are more difficult to design than ones that employ conventional in-phase power splitters, they do not, as in the latter case, inadvertently discard usable incident signal power. The concern, instead, is noise generated due to diplexer transmission losses. However, if the channel bandwidths are not so narrow as to produce significant losses, achievable noise performance will be superior to that of the alternative approach, which introduces equivalent attenuation at the input to each channel of 2–4 dB, depending on adopted in-phase power split ratio among channels. Narrow-bandwidth situations, where diplexer transmission losses may exceed these numbers, make the choice between contending variants more difficult, forcing a compromise between noise performance and immunity against out-of-band interference.

### III. EXPERIMENTAL TWO-BRANCH FILTERS

To demonstrate the practicability of the approach, two 10-GHz bandpass filters, one of each type, were designed and realized in hybrid-integrated-circuit form. Passive circuit components were implemented on 0.010-in-thick alumina substrates, with signal amplification provided by off-the-shelf microwave-monolithic integrated-circuit (MMIC) amplifier chips that were conveniently available. The frequency specifications for the two filters were not selected with any particular application in mind, merely to provide a useful basis for comparing the two variants.

With the focus on demonstrating feasibility, little attempt was made to devise systematic design methodologies. Rather, intuition and computer-aided techniques were relied on to arrive at representative solutions. The empirical procedures commenced with the selection of a passband center frequency, a passband width, and the positions of stopband-edge-defining transmission nulls. Channel bandpass candidates were then identified whose responses, if allowed to add in phase, would complement each other to establish well-behaved passband characteristics, while also exhibiting filter skirts that would intersect at designated null frequencies. The critical task was then to find actual channel filter structures that met these requirements, and supplied the necessary channel differential phase shift of  $360^\circ$  between null points. In each of the two experimental examples, the bulk of the phase shift was realized by adopting channel filter responses of different order, with fine adjustments to the differential phase shift accomplished with short pieces of uniform transmission

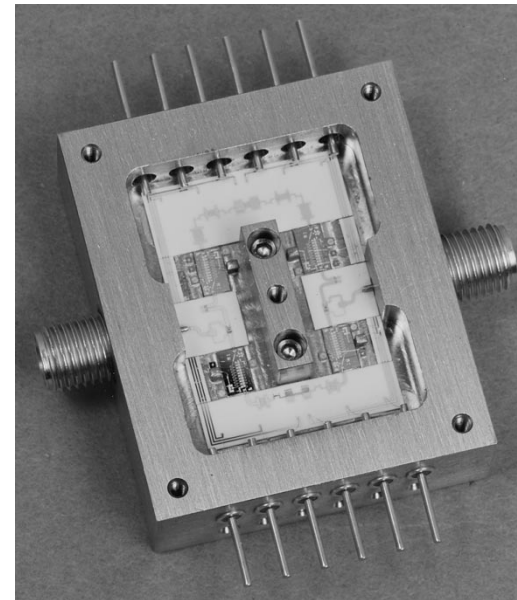


Fig. 3. First experimental 10-GHz two-branch channelized bandpass filter example, comprising an input power splitter, four MMIC amplifiers, two microstrip filter sections, and an output power combiner.

line. Final circuit configurations and parameter values were arrived at through iteration by acquiring accurate descriptions of key passive elements with the help of an electromagnetic-field solver, and employing standard numerical optimization techniques to seek solutions commensurate with stated objectives. Descriptions of the two-filter circuits and pertinent experimental observations are provided below.

#### A. Bandpass Filter with In-Phase Power Splitter and Combiner

The first filter example is based on the schematic block diagram of Fig. 1, involving two frequency-selective channels, connected in parallel with the help of an in-phase power splitter at the input and a symmetrically arranged power combiner at the output. A photograph of the experimental circuit is shown in Fig. 3. Each of the two network branches contains a pair of Texas Instruments Incorporated EG-8310 low-noise MMIC amplifiers separated by a lumped-element bandpass filter in microstrip form. The channel filters are similar in construction to ones described in the literature [5]. They are realized as cascade connections of capacitive  $\Pi$  networks and inductive short pieces of meander transmission line. Each  $\Pi$  network comprises a series-connected microstrip interdigital capacitor and two microstrip patches serving as shunt-connected capacitors to ground. Impedance transformations provided by these networks avoid a need for spiral-type inductors. To achieve the channel phase responses required for the two-branch scheme to work as intended, the channel filters are assigned second- and fourth-order responses, respectively. With reference to the photograph, the lower order filter comprises three of the mentioned capacitive  $\Pi$  networks and two inductive elements, whereas the higher order circuit contains a total of five capacitive  $\Pi$  networks and four inductive line segments. The lumped-element power splitter and combiner circuits are designed to be asymmetric, providing a cumulative amplitude offset of 2.8 dB between the two branches. The purpose of the offset is to

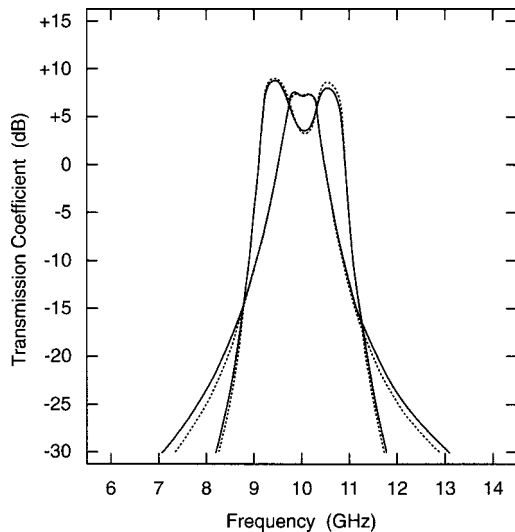


Fig. 4. Channel transmission responses of the first filter: — measured, - - - calculated.

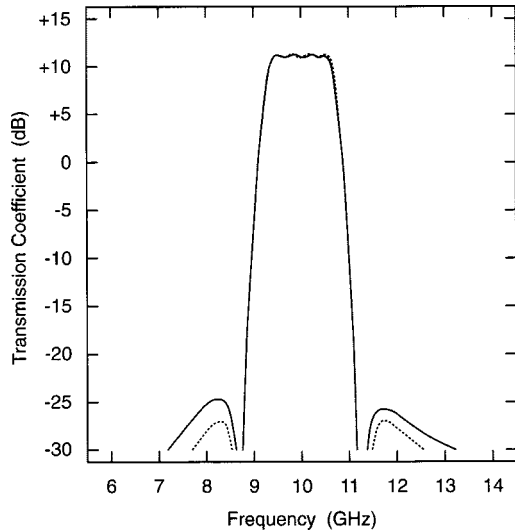


Fig. 5. Composite transmission response of the first filter: — measured, - - - calculated.

compensate for differences in loss characteristics between channel filters and permit optimum amplitude weighting of channel responses without the engagement of amplifier-based gain controls that can contribute excess noise.

The second- and fourth-order filters are both given double-tuned bandpass characteristics, but with different profiles. Measured and calculated amplitude responses for the two channels are depicted in Fig. 4. The measured curves were acquired by shutting off one channel at a time with the help of available amplifier gain controls. Changes in impedance-matching conditions introduced by engaging the controls appeared to have only minor effects on the measured results. The channel transfer characteristics, with associated phase responses designed to track each other across designated passband frequencies, combine through vector addition to produce quasi-elliptic composite-filter transfer characteristics with well-conditioned passband attributes, as shown in Fig. 5. (When comparing the results in Fig. 4 with those in Fig. 5,

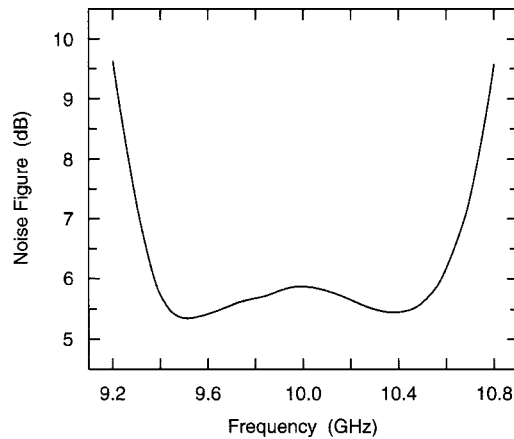


Fig. 6. Measured noise performance of the first filter.

it should be remembered that pertinent decibel values must be converted to linear voltage quantities prior to vector summation.) The two stopband-edge-defining transmission nulls coincide with the outlying crossover points of the two channel responses in Fig. 4. As is evident, the nulls are prominently involved in determining filter flank steepness.

The equal-ripple passband response was specifically selected to illustrate the process of synthesizing a composite bandpass response from two customized basis functions generated by the channel networks. The composite response could, just as easily, have been designed for maximum passband flatness or for best phase behavior. As in any filter situation, there are direct trade-offs among passband ripple, flank steepness, and stopband rejection. The optimum choice will depend on the application. To improve both flank selectivity and stopband rejection further, the easiest approach is to connect two-branch filters in cascade, rather than attempt to configure the base assembly with additional branches.

Noise is a common concern in microwave active filters. The concern relates especially to the passband edges, where attempts to sharpen them by selectively boosting signal transmission can lead to increased noise. In channelized filters, there are seldom surprises, though, due to the absence of regenerative feedback. With each channel composed of a simple cascade of amplifiers and passive filter sections, noise performance can be easily assessed. To illustrate this, the noise figure of the filter was measured as a function of frequency, and is plotted in Fig. 6. The response behaves as expected, based on a manufacturer-provided amplifier noise figure of 3.2 dB, and asymmetrically distributed channel excitations that fall below the incident signal level by 2.6 and 4.0 dB, respectively. Computer-generated estimates confirm that the input amplifiers and input power splitter are the main contributors to the overall noise figure, whereas channel filter losses and the output amplifiers account for only a few tenths of a decibel each. Due to the amount of incorporated channel amplification, noise generated by the output power combiner itself becomes negligible. As can be seen from Fig. 4, the two channels are designed to effect different regions of the passband response, with the fourth-order channel mostly responsible for the shoulder regions, and the second-order channel accountable for the mid-portion of the passband. The noise-figure hump in the band center is the

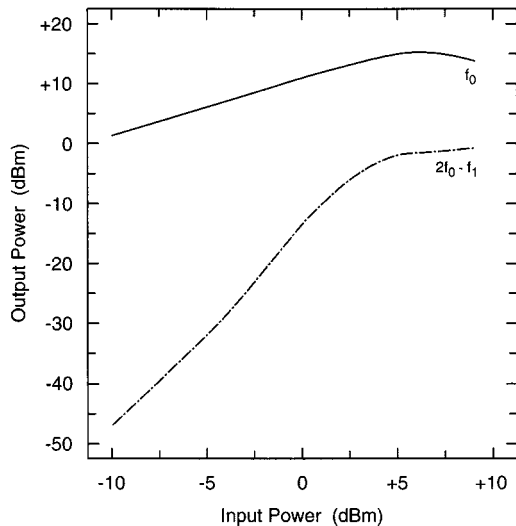


Fig. 7. Measured 9.5-GHz fundamental-frequency response of the first filter as a function of incident signal power, and associated two-tone third-order intermodulation response.

consequence of the unequally amplitude-weighted channels, as required to obtain an equal-ripple passband amplitude response without the use of amplifier gain controls.

Another concern with microwave active filters are signal by-products generated by active-device nonlinearities. To show that the current filter is also well behaved in this regard, the third-order intermodulation response was measured at the passband center and at both passband edges. The two-tone measurements were performed with a 10-MHz separation between excitation signals. The results, together with the corresponding fundamental-frequency responses of the filter, are plotted in Figs. 7–9. The curves are similar in appearance, with third-order intercept point readings of 25.8 dBm at the passband center to 24.4 dBm at each of the passband edges. Observed minor differences among curve shapes are a consequence of the deliberate unequal signal distribution between branches at the input. Second-harmonic distortion at the passband center was also measured and is recorded in Fig. 8. It is mainly attributed to nonlinearities associated with the channel output amplifiers, as contributions from the preamplifiers are constrained by channel frequency selectivity.

#### B. Bandpass Filter with Diplexer-Connected Branches

The second example relates to the schematic block diagram shown in Fig. 2. The implementation comprises a symmetric back-to-back arrangement of two frequency diplexer circuits, with a Texas Instruments Incorporated EG-8310 low-noise MMIC amplifier—the same type of chip employed in the previous case—used to link the ports of corresponding diplexer branches. A photograph of the circuit is provided in Fig. 10. Each microstrip diplexer circuit, in accordance with Fig. 2, comprises two bandpass filters joined at a common port, with one filter having a single-resonant response and the other exhibiting double-resonant behavior. The single-resonant circuit contains one inductive straight line segment flanked by two interdigital capacitive  $\Pi$  networks similar to those used in the previous example, whereas the double-resonant arm of the

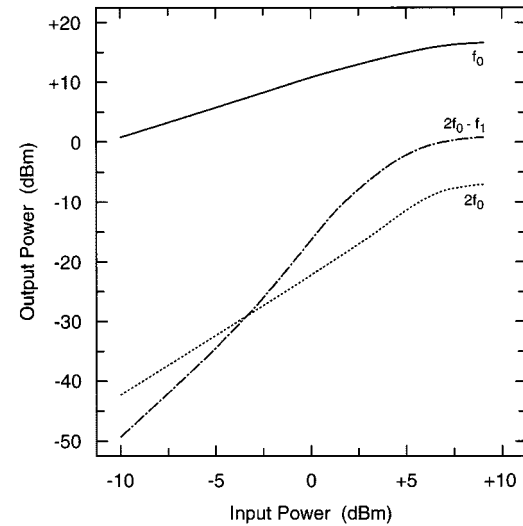


Fig. 8. Measured fundamental-frequency response of the first filter as a function of incident 10-GHz signal power, together with measured second-harmonic distortion and two-tone third-order intermodulation responses.

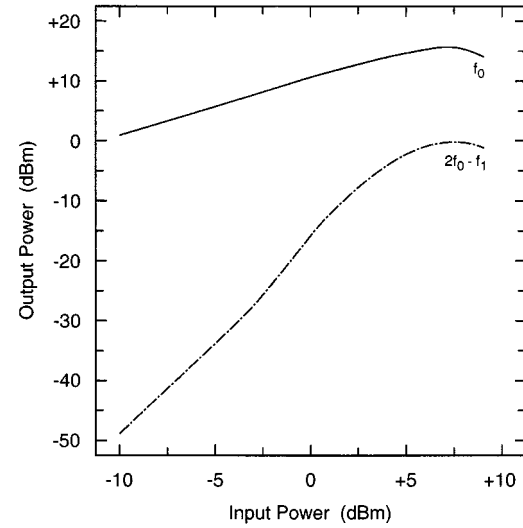


Fig. 9. Measured 10.5-GHz fundamental-frequency response of the first filter as a function of incident signal power, and associated two-tone third-order intermodulation response.

diplexer contains two inductive elements, three capacitive  $\Pi$  networks, and a transmission-line-based phase vernier. When operating in conjunction with each other, the corresponding diplexer branches define two filter channels whose responses differ by an aggregate of two orders, as in the first example.

A critical design task is that of parallel connecting the branches of each diplexer to realize an impedance-matched common port that can serve either as composite-filter input or output port. The situation differs from normal practice, as pointed out earlier, because the scheme calls for diplexed frequency bands to share frequency allocations within the composite filter's passband. The employed configuration joins the two branches of each diplexer at their common junction through a simple three-inductor T network that series-connects each diplexer branch filter to the junction through a short segment of

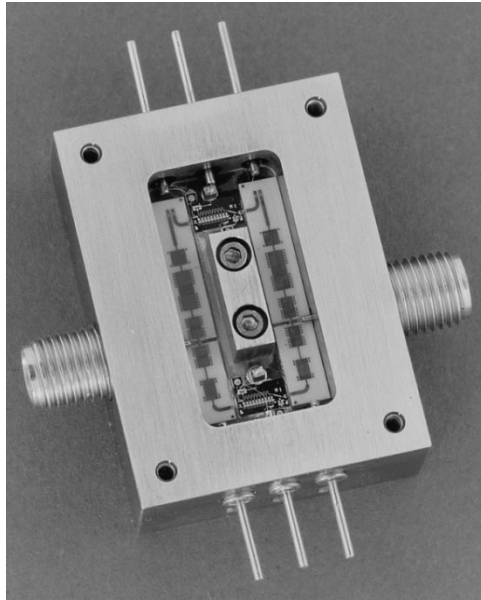


Fig. 10. Second experimental 10-GHz two-branch channelized bandpass filter example, comprising an input frequency diplexer, two MMIC amplifiers, and an output diplexer.

high-impedance transmission line, and complements this with a parallel-connected bond-wire inductor to ground at the junction point. The T-network inductors are conceptually part of the bandpass filter blocks shown in Fig. 2. The technique involves a tradeoff between achievable passband ripple, composite-filter selectivity, and common-junction return loss. Imposed on the current example is an arbitrarily selected design value of  $-20$  dB on the composite-filter input- and output-port return loss values.

Measured and calculated amplitude responses of the filter's two channels by themselves are plotted in Fig. 11. The measurements were again performed by shutting off gain stages, one at a time, with the help of available amplifier gain controls. Observed minor discrepancies between corresponding curves are largely attributed to control-induced changes in impedance-matching conditions at the amplifier ports. The effects are more apparent than in the first example, due to the inherent lack of signal isolation between filter channels. The composite filter's measured and calculated amplitude characteristics, with both channels activated, are presented in Fig. 12, and agree well. As can be seen, the designated transmission null positions again coincide with the frequency positions of the channel amplitude crossover points, yielding quasi-elliptic behavior. (When comparing the power-based results of Fig. 11 to those of Fig. 12, it should once more be noted that any apparent discrepancy among the sets of curves is due to the fact that the composite filter responses derive from the superposition of pertinent signal voltages, not signal power levels.)

The noise performance of the filter was also investigated, with measured noise figure values plotted in Fig. 13. The results are consistent with manufacturer-provided amplifier noise figure values and estimates of input diplexer transmission losses. Particularly noteworthy is the flatness of the curve throughout the filter's passband region. This underlines the diplexer's efficiency with which its frequency-selective

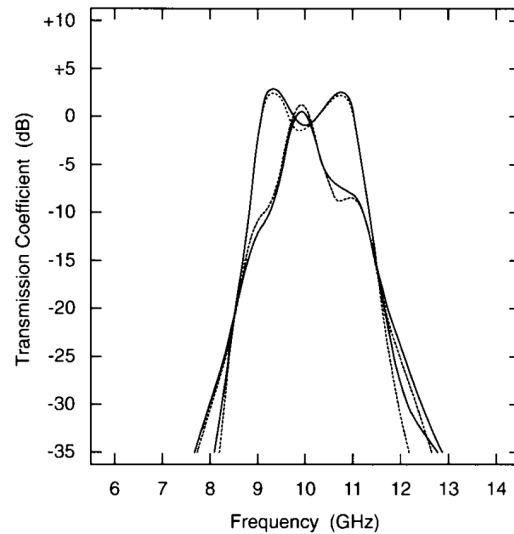


Fig. 11. Channel transmission responses of the second filter: — measured, - - - calculated.

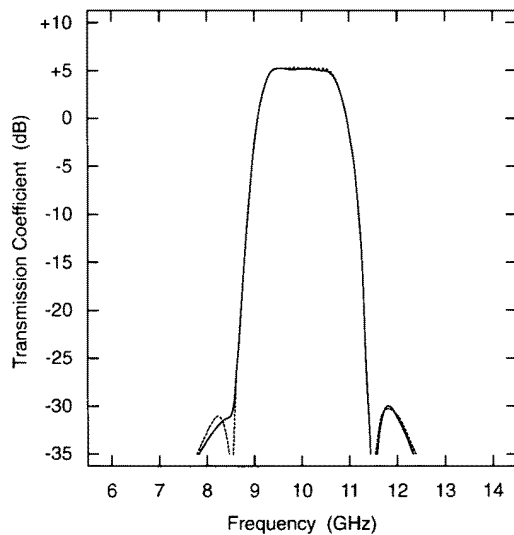


Fig. 12. Composite transmission response of the second filter: — measured, - - - calculated.

branch networks complement each other in establishing frequency-based signal distribution between channels at passband frequencies.

For the sake of completeness, the fundamental-frequency behavior of the filter together with its third-order-intermodulation and second harmonic distortion properties were measured as a function of incident signal power at band center. As anticipated, the results, which are given in Fig. 14, do not exhibit any unusual traits. The curves conform with those observed in the other example, after taking into account that the diplexer-based filter variant employs only one amplifier in each branch. Aside from a mid-band third-order intercept-point measurement of  $28.3$  dBm, which is  $2.5$  dB higher than in the first example, the main differentiating feature lies in the depressed values of second harmonic distortion. This is a direct result of out-of-band filtering action by the output diplexer circuit. Not shown here are the filter's

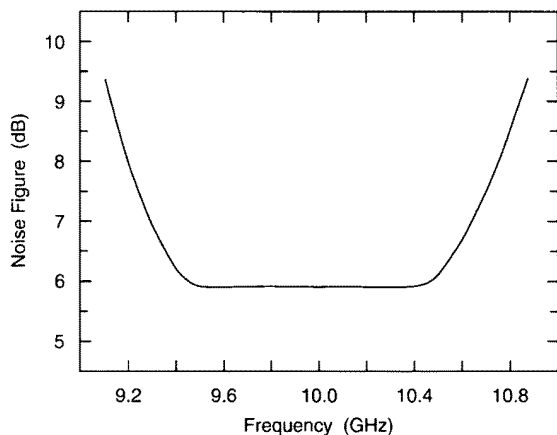


Fig. 13. Measured noise performance of the second filter.

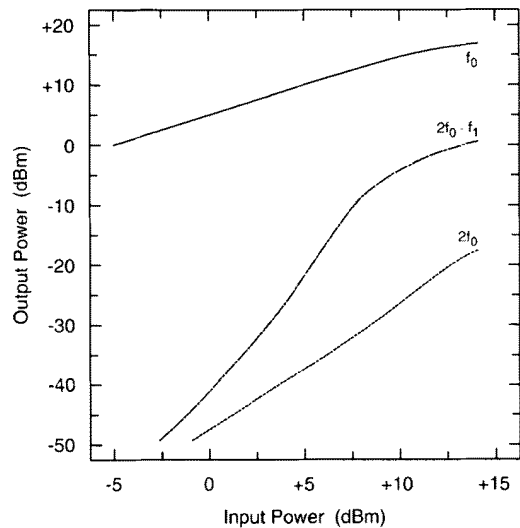


Fig. 14. Measured fundamental-frequency filter response of the second filter as a function of incident 10-GHz signal power, together with measured second-harmonic distortion and two-tone third-order intermodulation responses.

band-edge performance characteristics, which also match expectations.

#### IV. DISCUSSION

When comparing the described bandpass examples to more conventional three-branch realizations, the ability of a two-branch arrangement to win out over the latter with regard to physical size and noise performance is quite apparent. The localized contest between contending two-branch options, on the other hand, is less easily decided. Both have their distinct attributes, as alluded to earlier. The configuration that relies on a power-splitter-combiner pair to connect channel branches in parallel is easier to design and implement, whereas the dplexed-channel version offers frequency preselection that can prove helpful in situations where channel amplifiers risk performance degradation from out-of-band interference. In-band nonlinear circuit performance is mainly determined

by the active circuit components and is not an issue that necessarily favors one approach over the other. Noise behavior, in contrast, is substantially determined by losses associated with passive circuitry preceding the input amplifiers, giving rise to critical differences between the two options. By coincidence, the two experimental filters exhibit passband noise figures that fall within less than 1 dB of each other. The variant using the power-splitter-combiner arrangement would invariably have gained a noise advantage over the dplexer-based circuit, had narrower bandwidths or steeper filter flanks been sought, which would have increased dplexer transmission losses. The dplexer-based approach would still have retained the benefit of out-of-band signal pre- and post-selection, though, with the latter illustrated by the observed containment of second harmonic output.

An issue that is always of concern in filter applications is the sensitivity of filter performance characteristics to unintended changes in network parameters. This pertains particularly to active filters, where the inclusion of active-circuit elements tends to widen performance spreads due to semiconductor temperature dependencies and device manufacturing tolerances. Channelized filters, in general, are quite forgiving when it comes to reacting to such parameter changes, and the current examples are no exceptions. This attribute stems from the fact that the transfer characteristics of a channelized filter result from an amplitude-weighted superposition of conventional passive filter responses. Consequently, at frequencies where both channel responses reinforce each other, such as in the passband, or where one channel dominates, such as in outlying stopband areas, the amplitude response of the composite filter will be no more strongly affected by parameter changes than are individual channel responses by themselves. This includes changes in channel amplifier gain over temperature and time. At frequencies where cancellation between channel signals is sought for establishing transmission nulls, the effects of amplitude imbalances between channels can be more conspicuous. However, for a bandpass filter, whose precise null depth readings are often of subordinate significance, this, too, does not pose a real concern as long as stopband sidelobe levels are not unduly compromised in the process.

As for amplifier-induced variations in differential phase shift between channels, they have a tendency to skew the amplitude characteristics of the composite filter in a way that introduces a tilt to the passband plateau and adds asymmetry to the stopband sidelobes. The most visible impact, though, will again be on transmission null depth. Phase discrepancies must amount to a noticeable portion of the stipulated  $360^\circ$  channel differential phase shift between transmission null frequencies to be a major concern. The curves shown in Fig. 12 for the dplexed-channel filter can be used to illustrate what impact a mix of differential amplitude and phase deviations may have, pointing to a measured slight passband tilt and an incompletely articulated transmission null at the lower band edge. The observed discrepancies between measured and calculated results were actually created by a special circumstance that is unrelated to the issue of active-element involvement or the filter concept itself. The deviations from ideality are largely due to the inability of the employed commercial electromagnetic-field solver to predict the

characteristics of the passive diplexer circuits with accuracy and insufficient post-fabrication tuning provisions to accommodate the larger-than-expected errors.

Sensitivity to parameter changes is of special relevance when insuring against potential circuit instability. Channelized active filters are not prone to instability, due to their general reliance on feedforward-only signal flow. The amplifiers used to direct signal flow are never completely unilateral, though, allowing small amounts of unavoidable parasitic feedback to occur. Possible concerns can be easily countered by employing unconditionally stable gain stages and securing sufficient isolation between channels, as provided for in the first filter example. Indeed, the circuit did not exhibit the slightest tendency to support parasitic oscillation during extensive experimentation. If one of the two demonstration circuits was to be a possible candidate for supporting instabilities, it would have been the diplexer-based variant, with its intrinsic lack of isolation between channels at passband frequencies. However, even in the face of severe manipulation during post-fabrication tuning, which, out of curiosity, was carried well beyond what was actually required to achieve the reported results, no sign of instability in this circuit was observed.

## V. CONCLUSIONS

The two experimental circuits presented in this paper have demonstrated how microwave channelized active bandpass filters—like their low-pass, high-pass, and band-reject counterparts—can be implemented with only two feedforward branches. By going from an earlier three-branch configuration to a two-branch assembly, substantial overall size reductions are achieved, prime-power consumption is reduced, and noise performance is improved. The use of shared-frequency-band dippers, whose practicability has been confirmed by the second experimental example, appears particularly suited for applications where frequency preselection is desired.

The channelized active filter concept was originally developed to permit the realization of filters with good selectivity that could be implemented in planar form. Although the approach can handle fairly large passive-circuit losses, employing the lowest loss technology is always of advantage. Hence, depending on the application requirements, nonplanar implementations may be given consideration, such as a combination of dielectric-resonator technology and integrated amplifiers. Independent of the design option chosen, the resultant filter will invariably incorporate the benefits of the channelized architecture. Attributes relate not only to compactness, selectivity, circuit stability, noise behavior, and intermodulation performance achievable with readily available technologies, but also to the graceful degradation of filter characteristics with circuit element values changing over time, and the convenience of the modular de-

sign process. The described two-branch technique, in either of its presented forms, thus offers itself as a viable and attractive alternative to more commonly pursued filter miniaturization approaches.

## ACKNOWLEDGMENT

The author extends special thanks to W. Kruppa, Naval Research Laboratory, Washington, DC, for his constructive comments, to S. W. Kirchoefer, Naval Research Laboratory, for his valuable assistance with the assembly of the second test circuit, and to R. Oberle and E. Reese, Texas Instruments Incorporated, Dallas, TX, for providing the carefully characterized MMIC amplifier chips employed in both experiments. The amplifier chips were designed and fabricated by Texas Instruments Incorporated under the Defense Advanced Research Projects Agency MIMIC Program. The channelized active filter work was inspired by Navy system requirements.

## REFERENCES

- [1] P. Katzin, B. Bedard, and Y. Ayasli, "Narrow-band MMIC filters with automatic tuning and  $Q$ -factor control," in *IEEE MTT-S Int. Microwave Symp. Dig.*, vol. 1, June 1993, pp. 403–406.
- [2] C. Rauscher, "Microwave active filters based on transversal and recursive principles," *IEEE Trans. Microwave Theory Tech.*, vol. MTT-33, pp. 1350–1360, Dec. 1985.
- [3] M. J. Schindler and Y. Tajima, "A novel MMIC active filter with lumped and transversal elements," *IEEE Trans. Microwave Theory Tech.*, vol. 37, pp. 2148–2153, Dec. 1989.
- [4] C. Rauscher, "Microwave channelized active filters—A new modular approach to achieving compactness and high selectivity," *IEEE Trans. Microwave Theory Tech.*, vol. 44, pp. 122–132, Jan. 1996.
- [5] D. Swanson, "Thin-film lumped-element microwave filters," in *IEEE MTT-S Int. Microwave Symp. Dig.*, vol. 2, June 1989, pp. 671–674.



**Christen Rauscher** (S'73–M'75–SM'82–F'89) received the Diploma in electrical engineering and the Doctorate degree from the Swiss Federal Institute of Technology, Zürich, Switzerland, in 1969 and 1975, respectively.

From 1976 to 1978, he held an international fellowship from the Swiss National Science Foundation, under which he studied the nonlinear behavior of GaAs field-effect transistors at Cornell University, Ithaca, NY, and at the Naval Research Laboratory, Washington, DC. He subsequently joined the Naval Research Laboratory, as a Member of the Technical Staff, where he currently heads the Solid-State Circuits Section. On sabbatical leave from 1985 to 1986, he investigated the application of high-speed photoconductor technology to the on-chip characterization of microwave monolithic circuits and millimeter-wave devices at the Los Alamos National Laboratory, Los Alamos, NM. His current research interests remain centered on the pursuit of new high-frequency filter concepts and the exploitation of nonlinear signal interaction in semiconductor devices at microwave, millimeter-wave, and optical frequencies.

Dr. Rauscher is currently serving a three-year term as an IEEE Distinguished Microwave Lecturer. He was the recipient of the 1987 IEEE Microwave Prize, the 1991 Naval Research Laboratory Sigma Xi Applied Science Award presented by the Scientific Research Society of America, and the 1999 IEEE Microwave Application Award.